Claremont Colleges
Scholarship @ Claremont

HMC Senior Theses | HMC Student Scholarship

2021

Modelling the Transition from Homogeneous to Columnar States in Locust Hopper Bands

Miguel Velez

Follow this and additional works at: https://scholarship.claremont.edu/hmc_theses

 Part of the Dynamic Systems Commons, Non-linear Dynamics Commons, Numerical Analysis and Computation Commons, and the Ordinary Differential Equations and Applied Dynamics Commons

Recommended Citation

Velez, Miguel, "Modelling the Transition from Homogeneous to Columnar States in Locust Hopper Bands" (2021). *HMC Senior Theses*. 254.
https://scholarship.claremont.edu/hmc_theses/254

This Open Access Senior Thesis is brought to you for free and open access by the HMC Student Scholarship at Scholarship @ Claremont. It has been accepted for inclusion in HMC Senior Theses by an authorized administrator of Scholarship @ Claremont. For more information, please contact scholarship@cuc.claremont.edu.

Modelling the transition from homogeneous to columnar states in locust hopper bands

Miguel Velez

Andrew Bernoff, Advisor

Jasper Weinburd, Reader

Department of Mathematics

May, 2021

Copyright © 2021 Miguel Velez.

The author grants Harvey Mudd College and the Claremont Colleges Library the nonexclusive right to make this work available for noncommercial, educational purposes, provided that this copyright statement appears on the reproduced materials and notice is given that the copying is by permission of the author. To disseminate otherwise or to republish requires written permission from the author.

Abstract

Many biological systems form structured swarms, for instance in locusts, whose swarms are known as hopper bands. There is growing interest in applying mathematical models to understand the emergence and dynamics of these biological and social systems. We model the locusts of a hopper band as point particles interacting through repulsive and attractive social "forces" on a one dimensional periodic domain. The primary goal of this work is to modify this well studied modelling framework to be more biological by restricting repulsion to act locally between near neighbors, while attraction acts globally between all individuals. This is a biologically motivated assumption because repulsion in swarms is mainly a collision avoidance mechanism. We construct a discrete and continuum model in the limit of infinite individuals. Using an energy formulation of both discrete and continuum models, we find energy minimizing equilibrium configurations that are either constant density or clumped. Then, we perform a stability analysis of these swarm configurations to find transitions of stability and hysteresis. We show that with local repulsion and global attraction the constant density equilibrium has a bifurcation to instability for both the total mass of the swarm and the attraction strength of individuals.

Contents

Acknowledgments

Thank you to Professor Bernoff and Professor Weinburd who have supported me over the last year in working on this mathematics. Special thanks to Professor Bernoff who has both taught me in courses over the years and during our research together because he has contributed more so than anyone else to my mathematical ability. I appreciate Harvey Mudd College as an institution for making so much knowledge available to me and the HMC Mathematics Department in particular for fostering my Individual Program of Study in applied mathematics.

Chapter 1

Introduction

A swarm is a group of biological individuals that have emergent collective behaviors usually using simple interaction rules. Locusts, for example, organize themselves into planar fronts when food is abundant and into foraging columns when food is sparse to make consumption of resources most efficient. We are interested in the transition from homogeneous states to columnar states in these locusts; in other words, states in which the locusts are evenly spaced to states in which some are clumped together. This transition corresponds to the emergence of foraging columns in locust hopper bands.

In the case of collective motion, the interactions between individuals in the swarm can be modelled as "social forces" of attraction and repulsion. Because swarming individuals tend to have a strongly aligned direction of motion, we can reduce the problem to one dimension in which we consider the particles interacting perpendicular to the average direction of motion of the swarm. We treat social forces that are pairwise and additive such that the velocity of a particle is proportional to the sum of its interaction force with every other particle. Because locusts are large and experience strong drag forces relative to their weight, a first order model where force is proportional to velocity is justifiable.

Often, edge effects in swarms on an infinite line are ignored and we will do the same. To appropriately account for this, we assume the individuals in our model lie on a periodic boundary such that, as the swarm size becomes large, we can approximate well the behavior of swarms on an infinite line without edge effects. As is common in physics, we use an energy formulation of this problem to evaluate the stability of the evenly spaced configuration of particles. Because of the periodic boundary conditions, we are able to find

an analytical expression for the eigenvalues determining stability. Previous work detailed by Barth (2019), works through a numerical stability analysis of this model on periodic domain. Quentin shows where the model transitions from even spacing to clumped spacing between particles.

The discrete formulation of our swarming model has a continuum analogue that can be found by considering the limit of infinite number of individuals. As the number of individuals approaches infinity, an evenly spaced configuration of particles becomes a constant density solution to an energy functional. We use a framework developed by Bernoff and Topaz (2011) for transitioning from discrete to continuum formulations of the model and conduct a stability analysis on the resulting energy functional using calculus of variations. However, in biology, repulsion operates as a collision avoidance mechanism. For this reason, we later adapt our model such that only an individual's nearest neighbors interact repulsively while all particles interact attractively. With a continuum model of nearest neighbor repulsion, we test the stability of the constant density solution as the total mass of the swarm increases. Burger et al. (2014) investigate the properties of a continuum swarming model with local repulsion and so our analysis is inspired by and compared to their own.

We analyze the stability of both discrete and continuum models with two different repulsive potential energy functions, one Morse repulsion that acts globally between all individuals and a power-law with general exponent that is restricted to repel locally. Previous work on continuum swarming models shows that, with global repulsion, the stability of the constant density solution is independent of total mass. There are empirical reasons to believe that this is nonbiological. As the total mass of the swarm increases, the support of the swarm should increase to keep the density constant becoming unstable after some threshold of density is crossed. In locusts, higher densities are associated with the formation of columnar structures that we are modelling as clumping in one dimension.

Chapter 2

Discrete Formulation

2.1 Equations of motion

Consider N point particles interacting via a "social force" function, $q(r)$, of attraction and repulsion terms in one dimension. The position of each particle, x_i, changes according to a first order equation of motion proportional to the sum of all the interaction forces

$$\frac{dx_i}{dt} = \sum_{\substack{j=1 \\ j \neq i}}^{N} m q(x_i - x_j), \quad m = \frac{M}{N}, \tag{2.1}$$

where M is the total mass of all the particles in the system and m is a "social mass". The social mass ensures that the strength of the superposition of forces remains bounded as $N \to \infty$. If the force, $q(r)$, is an integrable function then we can rewrite the equations of motion as the negative gradient of a pairwise potential energy of each interaction. The pairwise potential energy is given by

$$Q(r) = -\int q(r)\, dr. \tag{2.2}$$

Under this assumption, the equations of motion can be rewritten to be

$$\frac{dx_i}{dt} = -m \sum_{\substack{j=1 \\ j \neq i}}^{N} \frac{\partial Q}{\partial x_i}(x_i - x_j). \tag{2.3}$$

In Chapter 4, we discuss in more detail the particular potential energy functions chosen for our numerical analyses but for now suppose that the potential energy $Q(r)$ is even and L-periodic such that $Q(-r) = Q(r)$ and $Q(r + L) = Q(r)$, where L is the length of the periodic interval.

2.2 Energy and Lattice stability

The total energy of the system is the superposition of all pairwise interactions excluding self-interaction,

$$E(\vec{x}) = \frac{1}{2} \sum_{i=1}^{N} \sum_{\substack{j=1 \\ j \neq i}}^{N} m^2 \tilde{Q}(x_i - x_j). \tag{2.4}$$

In the case of an evenly spaced equilibrium configuration, we can define the spacing between particles to be $\Delta = \frac{L}{N}$, such that agents have equilibrium position $x_i^* = i\Delta$ for $i \in \{1, 2, 3, ..., N\}$. We use the Taylor expansion of the energy to determine stability information of the equilibrium $\vec{x}^*$ such that $\vec{x} = \vec{x}^* + \vec{\gamma}$ where $\vec{\gamma}$ is a vector of perturbations to each of the agent's position. The Taylor expansion is

$$E(\vec{x}) \approx E(\vec{x}^*) + \vec{\gamma}^T \nabla E(\vec{x}^*) + \frac{1}{2} \vec{\gamma}^T \mathbf{H} \vec{\gamma} \tag{2.5}$$

$$\approx E(\vec{x}^*) + \sum_{j=1}^{N} \frac{\partial E(\vec{x}^*)}{\partial x_j} \gamma_j + \frac{1}{2} \sum_{i=1}^{N} \sum_{j=1}^{N} \frac{\partial^2 E(\vec{x}^*)}{\partial x_j \partial x_i} \gamma_j \gamma_i, \tag{2.6}$$

where the Hessian matrix is defined by

$$\mathbf{H}_{ij} \equiv \frac{\partial^2 E(\vec{x}^*)}{\partial x_j \partial x_i}.$$

By the second partial derivative test, the eigenvalues of the Hessian matrix at equilibrium determine the linear stability of the system. If the set of eigenvalues are positive definite, the equilibrium is stable and it is unstable otherwise. To gain some intuition, note that by the definition of an equilibrium point, $\frac{\partial E}{\partial x_j} = 0$ for all $j \in \{1, 2, 3, ..., N\}$ and we can rearrange Equation 2.6 to find an expression for the change in energy caused by the perturbation

$$E(\vec{x}) - E(\vec{x}^*) \approx \frac{1}{2} \vec{\gamma}^T \mathbf{H} \vec{\gamma}. \tag{2.7}$$

If the energy increases for any possible perturbation, this is an indication that the point is a stable minimum. Suppose the perturbation is the kth eigenvector $\vec{v}^{(k)}$ of $\mathbf{H}$ with corresponding eigenvalue $\lambda^{(k)}$, then the change in energy of the system is

$$E(\vec{x}) - E(\vec{x}^*) \approx \frac{1}{2}\lambda^{(k)}|\vec{v}^{(k)}|^2. \tag{2.8}$$

If the set of eigenvalues is positive definite, then the change in energy following any arbitrary perturbation is positive because any arbitrary vector can be expressed in terms of the eigenbasis of the Hessian. If there is even one negative eigenvalue then there exists a perturbation that can lower the energy further by moving away from equilibrium suggesting that the equilibrium is an unstable maximum.

2.3 Analysis of Hessian

The Hessian is a matrix of second derivatives of our total energy function. To arrive at an analytical expression for the eigenvalues of our Hessian, we need to derive it in terms of a pairwise interaction potential energy function. We will begin by computing its first derivative:

$$\begin{aligned}
\frac{\partial E}{\partial x_k} &= \frac{\partial}{\partial x_k}\frac{1}{2}\sum_{i=1}^{N}\sum_{\substack{j=1\\ j\neq i}}^{N} m\tilde{Q}(x_i - x_j), \\
&= \frac{m}{2}\sum_{i=1}^{N}\sum_{\substack{j=1\\ j\neq i}}^{N}\frac{\partial}{\partial x_k}\tilde{Q}(x_i - x_j), \\
&= \frac{m}{2}\sum_{i=1}^{N}\sum_{\substack{j=1\\ j\neq i}}^{N}\left[\frac{\partial\tilde{Q}}{\partial x_k}\delta_{ik} - \frac{\partial\tilde{Q}}{\partial x_k}\delta_{jk}\right], \\
&= \frac{m}{2}\left[\sum_{\substack{j=1\\ j\neq k}}^{N}\frac{\partial\tilde{Q}(x_k - x_j)}{\partial x_k} - \sum_{\substack{i=1\\ i\neq k}}^{N}\frac{\partial\tilde{Q}(x_i - x_k)}{\partial x_k}\right].
\end{aligned}$$

Because the summations are independent of one another, we can use that $\tilde{Q}'(r)$ is an odd function and $-\tilde{Q}'(-r) = \tilde{Q}(r)$ to reindex the problem such

that $i \to j$. Then,

$$\begin{aligned}\frac{\partial E}{\partial x_k} &= \frac{m}{2}\Bigg[\sum_{\substack{j=1\\ j\neq k}}^{N}\frac{\partial \tilde{Q}(x_k - x_j)}{\partial x_k} + \sum_{\substack{j=1\\ j\neq k}}^{N}\frac{\partial \tilde{Q}(x_k - x_j)}{\partial x_k}\Bigg] \\ &= m\sum_{\substack{j=1\\ j\neq k}}^{N}\frac{\partial \tilde{Q}(x_k - x_j)}{\partial x_k}. \end{aligned} \tag{2.9}$$

Notice that Equation 2.9 shows that our equations of motion define a dynamical system flowing along the negative gradient of the total energy. Now, we can compute the Hessian as follows:

$$\begin{aligned}\mathbf{H}_{ik} &= \frac{\partial}{\partial x_i}\frac{\partial E}{\partial x_k}, \\ &= m\frac{\partial}{\partial x_i}\sum_{\substack{j=1\\ j\neq k}}^{N}\tilde{Q}'(x_k - x_j), \\ &= m\sum_{\substack{j=1\\ j\neq k}}^{N}\tilde{Q}''(x_k - x_j)\frac{\partial}{\partial x_i}\big[x_k - x_j\big], \\ &= m\sum_{\substack{j=1\\ j\neq k}}^{N}\tilde{Q}''(x_k - x_j)\big[\delta_{ki} - \delta_{ji}\big], \\ &= m\Bigg[\delta_{ki}\sum_{\substack{j=1\\ j\neq k}}^{N}\tilde{Q}''(x_k - x_j)\Bigg] - m\tilde{Q}''(x_k - x_i). \end{aligned}$$

This can be rewritten such that one term is a constant that defines the values of the matrix along the diagonal and the other is matrix of off-diagonal terms. Evaluated at equilibrium with positions $x_i^* = i\Delta$, the Hessian becomes

$$\mathbf{H}_{ij} = m\delta_{ij}\sum_{\substack{k=1\\ k\neq j}}^{N}\tilde{Q}''\Big(\Delta(j-k)\Big) - m(1-\delta_{ij})\tilde{Q}''\Big(\Delta(j-i)\Big). \tag{2.10}$$

So, we define

$$P \equiv \sum_{k=1}^{N-1} \tilde{Q}''(k\Delta), \qquad S_{ij} \equiv -\tilde{Q}''\left(\Delta(i-j)\right),$$

such that,

$$\mathbf{H}_{ij} = \delta_{ij}P + (1-\delta_{ij})S_{ij}.$$

The Hessian is symmetric and circulant because of the symmetry of second derivatives and the periodicity of the problem. The diagonal matrix P is trivially circulant and S_{ij} is circulant because $\tilde{Q}''(r)$ is an even and periodic function. The advantage of working with a circulant matrix is that the eigenvalues can be found regardless of eigenvectors.

2.4 On circulant matrices

A circulant matrix is defined as a square $N \times N$ matrix that is fully specified by the first row vector, $\vec{h}$, where each subsequent row is a cyclic permutation of this vector. Colloquially, this means that every row is the same except every element is shifted to the right by one. Consider a circulant matrix $\mathbf{H}$,

$$\mathbf{H} = \begin{bmatrix} h_1 & h_2 & h_3 & \cdots & h_N \\ h_N & h_1 & h_2 & \cdots & h_{N-1} \\ h_{N-1} & h_N & h_1 & \cdots & h_{N-2} \\ \vdots & \vdots & \vdots & \ddots & \vdots \\ h_2 & h_3 & h_4 & \cdots & h_1 \end{bmatrix}.$$

The first eigenvector and eigenvalue pair, $\vec{v}^{(1)}$ and $\lambda^{(1)}$, are attainable by inspection. Suppose $\vec{v}^{(1)}$ is an $N \times 1$ vector of one's such that,

$$\mathbf{H}\vec{v}^{(1)} = \begin{bmatrix} h_1 & h_2 & h_3 & \cdots & h_N \\ h_N & h_1 & h_2 & \cdots & h_{N-1} \\ \vdots & \vdots & \vdots & \ddots & \vdots \\ h_2 & h_3 & h_4 & \cdots & h_1 \end{bmatrix} \begin{bmatrix} 1 \\ 1 \\ \vdots \\ 1 \end{bmatrix} = (h_1 + \cdots + h_N)\vec{v}^{(1)} = \lambda^{(1)}\vec{v}^{(1)}. \quad (2.11)$$

So, we know $\lambda^{(1)} = (h_1 + h_2 + \cdots + h_N)$. All the eigenvectors are expressible in terms of roots of unity. The N^{th} root of unity is defined by $\omega_N = e^{\frac{2\pi i}{N}}$ which creates a periodic set of complex numbers that yield 1 when raised to

the power N. The exponents of ω_N are periodic such that $\omega_N^{j+N} = \omega_N^j$. So, the kth eigenvector is given by,

$$\vec{v}^{(k)} = \begin{bmatrix} \omega_N^k \\ \omega_N^{2k} \\ \omega_N^{3k} \\ \vdots \\ \omega_N^{Nk} \end{bmatrix}.$$

Now we will derive an expression for the eigenvalues of a general circulant matrix. Consider a set of vectors defined by,

$$\vec{y}^{(k)} = \mathbf{H}\vec{v}^{(k)} = \begin{bmatrix} h_1 & h_2 & h_3 & \cdots & h_N \\ h_N & h_1 & h_2 & \cdots & h_{N-1} \\ \vdots & \vdots & \vdots & \ddots & \vdots \\ h_2 & h_3 & h_4 & \cdots & h_1 \end{bmatrix} \begin{bmatrix} \omega_N^k \\ \omega_N^{2k} \\ \vdots \\ \omega_N^{Nk} \end{bmatrix} = \begin{bmatrix} \sum_{j=1}^N h_j \omega_N^{jk} \\ \sum_{j=1}^N h_{(j-1)} \omega_N^{jk} \\ \sum_{j=1}^N h_{(j-2)} \omega_N^{jk} \\ \vdots \\ \sum_{j=1}^N h_{(j-N+1)} \omega_N^{jk} \end{bmatrix}.$$

To make things clearer, we will work with the ℓ^{th} element of the vector $\vec{y}^{(k)}$ which is given by,

$$\begin{aligned} \vec{y}_\ell^{(k)} &= \sum_{j=1}^N h_{(j-\ell)} \omega_N^{jk} = \sum_{j=1}^N h_{(j-\ell)} \left(\omega_N^{\ell k} \cdot \omega_N^{(j-\ell)k} \right) \\ &= \omega_N^{\ell k} \left(\sum_{j=1}^N h_{(j-\ell)} \omega_N^{(j-\ell)k} \right). \end{aligned}$$

Because the indices are periodic and the sum independent of ℓ, we can re-index ℓ out of the sum $(j - \ell) \longrightarrow j$ and the expression becomes,

$$\vec{y}_\ell^{(k)} = \omega_N^{\ell k} \left(\sum_{j=1}^N h_j \omega_N^{jk} \right) = \vec{v}_\ell^{(k)} \left(\sum_{j=1}^N h_j \omega_N^{jk} \right) = \vec{v}_\ell^{(k)} \lambda^{(k)}. \tag{2.12}$$

Finally we see that,

$$\lambda^{(k)} = \sum_{j=1}^N h_j \omega_N^{jk}. \tag{2.13}$$

This result is significant because the eigenvalues are computable using the Discrete Fourier Transform (DFT) matrix,

$$\mathbf{F} = \left[\vec{v}^{(1)}, \vec{v}^{(2)}, \vec{v}^{(3)}, \cdots, \vec{v}^{(N)}\right].$$

Multiplying a vector of first row elements, $\vec{h}$, by the DFT matrix we obtain a vector of eigenvalue elements such that,

$$\mathbf{F}\vec{h} = \begin{bmatrix} \omega_N^{11} & \omega_N^{12} & \omega_N^{13} & \cdots & \omega_N^{1N} \\ \omega_N^{21} & \omega_N^{22} & \omega_N^{23} & \cdots & \omega_N^{2N} \\ \omega_N^{31} & \omega_N^{32} & \omega_N^{33} & \cdots & \omega_N^{3N} \\ \vdots & \vdots & \vdots & \ddots & \vdots \\ \omega_N^{N1} & \omega_N^{N2} & \omega_N^{N3} & \cdots & \omega_N^{NN} \end{bmatrix} \begin{bmatrix} h_1 \\ h_2 \\ h_3 \\ \vdots \\ h_N \end{bmatrix} = \begin{bmatrix} \lambda^{(1)} \\ \lambda^{(2)} \\ \lambda^{(3)} \\ \vdots \\ \lambda^{(N)} \end{bmatrix} = \vec{\lambda}.$$

Much of this theory can be found in the work Karner et al. (2003).

2.5 Eigenvalues of Hessian matrix

Now knowing how to find the eigenvalues of a circulant matrix, we come back to the Hessian defined in Equation 2.10. As a reminder, the Hessian is

$$\mathbf{H} = \begin{bmatrix} P & -\tilde{Q}''\Big(-\Delta\Big) & -\tilde{Q}''\Big(-2\Delta\Big) & \cdots & -\tilde{Q}''\Big((1-N)\Delta\Big) \\ -\tilde{Q}''\Big(\Delta\Big) & P & -\tilde{Q}''\Big(-\Delta\Big) & \cdots & -\tilde{Q}''\Big((2-N)\Delta\Big) \\ -\tilde{Q}''\Big(2\Delta\Big) & -\tilde{Q}''\Big(\Delta\Big) & P & \cdots & -\tilde{Q}''\Big((3-N)\Delta\Big) \\ \vdots & \vdots & \vdots & \ddots & \vdots \\ -\tilde{Q}''\Big((N-1)\Delta\Big) & -\tilde{Q}''\Big((N-2)\Delta\Big) & -\tilde{Q}''\Big((N-3)\Delta\Big) & \cdots & P \end{bmatrix}.$$

Because $\tilde{Q}''(r)$ is an even L-periodic function and the particles are evenly distributed throughout the period at equilibrium, we know that $\tilde{Q}''((j-N)\Delta) = \tilde{Q}''(j\Delta) = \tilde{Q}''(-j\Delta)$ making it a circulant matrix. Now, we can use the DFT and the first row of our Hessian to find its eigenvalues. To make the eigenvalue calculation simpler, we must reindex the exponents of the roots of unity. Because they are N-periodic, we can rewrite the DFT matrix

such that,

$$\mathbf{F} = \begin{bmatrix} \omega_N^{00} & \omega_N^{01} & \omega_N^{02} & \cdots & \omega_N^{0(N-1)} \\ \omega_N^{10} & \omega_N^{11} & \omega_N^{12} & \cdots & \omega_N^{1(N-1)} \\ \omega_N^{20} & \omega_N^{21} & \omega_N^{22} & \cdots & \omega_N^{2(N-1)} \\ \vdots & \vdots & \vdots & \ddots & \vdots \\ \omega_N^{(N-1)0} & \omega_N^{(N-1)1} & \omega_N^{(N-1)2} & \cdots & \omega_N^{(N-1)(N-1)} \end{bmatrix}.$$

Now, multiplying $\mathbf{F}$ by the first row $\vec{h}$ of $\mathbf{H}$, the k^{th} eigenvalue is

$$\lambda^{(k)} = P\omega_N^{0k} - \tilde{Q}''(-\Delta)\omega_N^{1k} - \tilde{Q}''(-2\Delta)\omega_N^{2k} - \cdots - \tilde{Q}''((2-N)\Delta)\omega_N^{(N-2)k} - \tilde{Q}''((1-N)\Delta)\omega_N^{(N-1)k}$$

As stated in Section 2.4, the exponents of ω_N are N-periodic such that $\omega_N^{jk} = \omega_N^{(N-j)k}$. This allows us to combine many of the terms of $\lambda^{(k)}$. For example, the jth term after P and the jth term from the end can be reduced as follows:

$$\begin{aligned} -\tilde{Q}''(j\Delta)\omega_N^{jk} - \tilde{Q}''((j-N)\Delta)\omega_N^{(N-j)k} &= -\tilde{Q}''(j\Delta)\omega_N^{jk} - \tilde{Q}''((j-N)\Delta)\omega_N^{-jk} \\ &= -\tilde{Q}''(j\Delta)\left[\omega_N^{jk} + \omega_N^{-jk}\right] \\ &= -\tilde{Q}''(j\Delta)\left[e^{\frac{2\pi jk}{N}i} + e^{-\frac{2\pi jk}{N}i}\right] \\ &= -\tilde{Q}''(j\Delta)\left[2\cos\left(\frac{2\pi jk}{N}\right)\right] \end{aligned}$$

As long as N is an odd integer, there will be an even number of terms to pair and every term after P will be simplified in this way. For this reason, we assume from here onward that N is an odd integer to obtain a concise expression of eigenvalues that can be numerically evaluated. The resulting expression assuming an odd integer N is

$$\begin{aligned} \lambda^{(k)} &= P - 2\tilde{Q}''(\Delta)\cos\left(\frac{2\pi k}{N}\right) - \cdots - 2\tilde{Q}''\left(\frac{N-1}{2}\Delta\right)\cos\left(\frac{2\pi\frac{N-1}{2}k}{N}\right) \\ &= P - 2\sum_{\ell=1}^{(N-1)/2} \tilde{Q}''(\ell\Delta)\cos\left(\frac{2\pi\ell k}{N}\right) \end{aligned} \tag{2.14}$$

Now we re-index the problem such that, $N = 2M + 1$ and instead the agents' positions are $x_i^* = i\Delta$ where $i \in \{-M, -M+1, .., M\}$. Now the eigenvalues for an odd number of individuals are given by

$$\lambda^{(k)} = P - 2\sum_{\ell=1}^{M} \tilde{Q}''(\ell\Delta)\cos\left(\frac{2\pi\ell k}{N}\right) \quad k \in \{-M, -M+1, ..., M\}. \tag{2.15}$$

2.6 Symmetries of the system

Now, I will describe the implications of other symmetries of the system from a classical mechanics perspective. A symmetry of a system is defined by a transformation that leaves the action of the system unchanged. An action in physics is a functional that is the time integral of the Lagrangian of the system. Given a mechanical system with N generalized coordinates, x_i for $i \in \{1, 2, 3, ..., N\}$ or $\mathbf{x}$, the Lagrangian and the corresponding action respectively are:

$$L = T - U,$$
$$S[\mathbf{x}(t)] = \int_{t_a}^{t_b} L(t, \mathbf{x}, \dot{\mathbf{x}})\, dt,$$

where T is the total kinetic energy of the particles and U is the total potential energy due to the system's social forces. In classical mechanics, the dynamics of the system is governed by the function $\mathbf{x}(t)$ that makes the action stationary. Consider a transformation to each coordinate such that $x_i' = x_i + C$. Kinetic energy depends on $\dot{\mathbf{x}}$ and the potential energy depends on the distance between particles $|x_i - x_j|$, both of which are invariant under the transformation. Because the Lagrangian is unchanged by the transformation so is the action and our system is transitionally invariant. As a consequence, if the system is shifted along the real line by a constant, the energy of the system remains unchanged as well. As was demonstrated in Section 2.4, a vector $\vec{v}^{(1)}$ of ones is always an eigenvector of a circulant matrix. By Equation 2.8, the symmetry means that the corresponding eigenvalue $\lambda^{(1)}$ is equal to zero,

$$\lambda^{(1)} = h_1 + h_2 + \cdots + h_N = P - 2\sum_{\ell=1}^{M} \tilde{Q}''(\ell\Delta) = 0.$$

This result confirms our original definition of P in Section 2.3 and gives us a constraint on our numerical results. Every row and column of our Hessian matrix individually sums to zero. The expression for the k^{th} eigenvalue becomes,

$$\lambda^{(k)} = 2\sum_{\ell=1}^{M} \tilde{Q}''(\ell\Delta)\Big(1 - \cos\Big(\frac{2\pi}{N}\ell k\Big)\Big). \tag{2.16}$$

Chapter 3

Continuum Formulation

3.1 Discrete energy

So far, we have considered a general potential, $\tilde{Q}(r)$, where the repulsive and attractive contributions apply to each pair of individuals. For biological swarms, however, repulsion functions as a collision avoidance mechanism and thus only acts locally. In our continuum model derivation, we ensure that any repulsive potential energy chosen only acts on the nearest neighbors of any focal individual. To account for this, we rewrite our discrete model in such a way that repulsion only acts locally. We separate $\tilde{Q}(r)$ into two potentials such that

$$\tilde{Q}(r) = R(r) + A(r), \tag{3.1}$$

where $R(r)$ is a repulsive potential energy and $A(r)$ is an attractive potential energy. Consequently, we define the energy contribution of particle j by

$$e_j(\vec{x}) = \frac{1}{2}\left[R\left(\frac{\Delta_j^+}{h}\right) + R\left(\frac{\Delta_j^-}{h}\right)\right] + \frac{1}{2}\sum_{i=1}^{N} mA(x_j - x_i), \tag{3.2}$$

where the constant $h = \frac{L}{N}$ is the average distance between particles, $\Delta_j^+ = (x_{j+1} - x_j)$, and $\Delta_j^- = (x_j - x_{j-1})$. The factors h in $R(r)$ and m multiplied to $A(r)$ ensure that repulsion and attraction remain bounded as N approaches infinity. We find the total energy by summing over all individual energies

such that

$$E(\vec{x}) = \sum_{j=1}^{N} m e_j(\vec{x}) = \sum_{j=1}^{N} \frac{m}{2}\left[R\left(\frac{\Delta_j^+}{h}\right) + R\left(\frac{\Delta_j^-}{h}\right)\right] + \sum_{i=1}^{N}\sum_{\substack{j=1 \\ j\neq i}}^{N} \frac{m^2}{2} A(x_i - x_j) \quad (3.3)$$

3.2 Discrete to continuum

To derive the analogue continuum model, we define a discrete mass density function

$$\rho_d(x) = \sum_{i=1}^{N} m\delta(x - x_i)\, dx,$$

where each particle of mass m has position x_i. The δ-function is defined by

$$\delta(x) = \begin{cases} 1 & x = 0, \\ 0 & otherwise. \end{cases}$$

Using the discrete density $\rho_d(x)$, we find the cumulative density function to be

$$\Psi_d(x) = \begin{cases} 0 & x < x_1 \\ m[1/2 + (i-1)] & x = x_i, i = 1, ..., N \\ im & x_i < x < x_{i+1}, i = 1, ..., N \\ M & x > x_N, \end{cases}$$

where we have used the convention that integrating up to a δ-function yields half the mass of integrating through it. To establish correspondence between discrete and continuum models, we constrain $\Psi_d(x_i) = \Psi_c(x_i)$ where $\Psi_c(x)$ is a continuous cumulative density function,

$$\Psi_c(x) = \int_0^x \rho(x)\, dx,$$

and $\rho(x)$ is the continuous density of the swarm. As $N \to \infty$ for a fixed value of M, $\Psi_d(x)$ converges to $\Psi_c(x)$. Now, we will go through the derivation of the continuum energy term by term. First consider the attractive term,

$$E^A(\vec{x}) = \sum_{i=1}^{N}\sum_{\substack{j=1 \\ j\neq i}}^{N} \frac{m^2}{2} A(x_i - x_j).$$

By the cumulative density we know,

$$m = \Psi_c(x_{i+1}) - \Psi_c(x_i) = \int_{x_i}^{x_{i+1}} \rho(x)\,dx \approx \rho(x_i)\Delta_i^+, \tag{3.4}$$

where the approximation comes from a Riemann sum. Using the approximation we can rewrite the attractive energy,

$$E^A(\vec{x}) = \frac{1}{2}\sum_{i=1}^{N}\sum_{\substack{j=1\\ j\neq i}}^{N} \rho(x_i)\rho(x_j)A(x_i - x_j)\Delta_i^+\Delta_j^+.$$

We take the limit of infinite particles where both sums turn into integrals and the attractive energy function turns into an attractive energy functional,

$$\lim_{N\to\infty} E^A(\vec{x}) = W^A[\rho(x)] = \frac{1}{2}\int_0^L \int_0^L \rho(x)\rho(y)A(x-y)\,dxdy. \tag{3.5}$$

Now we will consider the repulsive energy and its continuum limit. Using Equation 3.4, the repulsive energy can be reformulated,

$$\begin{aligned} E^R(\vec{x}) &= \frac{1}{2}\sum_{j=1}^{N} m\left[R\Big(\frac{\Delta_j^+}{h}\Big) + R\Big(\frac{\Delta_j^-}{h}\Big)\right] \\ &= \frac{1}{2}\sum_{j=1}^{N} \frac{M}{N}\left[R\Big(\frac{M}{L\rho(x_j)}\Big) + R\Big(\frac{M}{L\rho(x_j)}\Big)\right] \\ &= \sum_{j=1}^{N} \frac{M}{L} R\Big(\frac{M}{L\rho(x_j)}\Big)h. \end{aligned}$$

In the limit of infinite N, h becomes an infinitesimal such that,

$$\lim_{N\to\infty} E^R(\vec{x}) = W^R[\rho(x)] = \sigma\int_0^L R\Big(\frac{\sigma}{\rho(x)}\Big)\,dx, \tag{3.6}$$

where $\sigma = \frac{M}{L}$ is the average density of the swarm. Finally, the complete continuum energy in functional form is given by,

$$W[\rho(x)] = \sigma\int_0^L R\Big(\frac{\sigma}{\rho(x)}\Big)\,dx + \frac{1}{2}\int_0^L\int_0^L \rho(x)\rho(y)A(x-y)\,dxdy. \tag{3.7}$$

3.3 Linear stability of homogeneous density

We use variational calculus to determine whether a constant density solution is a minimizer of our energy functional, $W[\rho(x)]$. Let

$$\rho(x) = \bar{\rho} + \epsilon\tilde{\rho}(x), \tag{3.8}$$

where $\bar{\rho}$ is a constant density solution of total mass M and $\epsilon\tilde{\rho}(x)$ is a zero mass perturbation. We can expand the functional such that,

$$W[\rho(x)] \approx W[\bar{\rho}] + \epsilon W_1[\bar{\rho}, \tilde{\rho}] + \epsilon^2 W_2[\bar{\rho}, \tilde{\rho}], \tag{3.9}$$

where W_1 is the first variation and W_2 the second variation. For $\bar{\rho}$ to be an equilibrium solution the first variation must equal zero and, for that equilibrium to be a stable minimizer, the second variation must be greater than zero.

The first variation is given by,

$$\begin{aligned} W_1[\bar{\rho}, \tilde{\rho}] &= -\int_0^L \frac{\tilde{\rho}(y)\sigma^2}{\bar{\rho}(y)^2} R'\Big(\frac{\sigma}{\bar{\rho}(y)}\Big)\, dy + \int_0^L \tilde{\rho}(y) \int_0^L \bar{\rho}(x) A(x-y)\, dx dy \\ &= \int_0^L \tilde{\rho}(y)\Big[\int_0^L \bar{\rho}(x) A(x-y)\, dx - \frac{\sigma^2}{\bar{\rho}(y)^2} R'\Big(\frac{\sigma}{\bar{\rho}(y)}\Big)\Big]\, dy. \end{aligned} \tag{3.10}$$

Because $\tilde{\rho}(y)$ is a zero mass perturbation, its integral over the period $[0, L]$ is zero. As long as the bracketed portion of Equation 3.10 is a constant, then the first variation is equal to zero. Moreover, if the bracketed expression is not constant then one can find a perturbation such that the first variation is nonzero indicating that the solution is not an equilibrium of the system. For $W_1[\bar{\rho}, \tilde{\rho}] = 0$,

$$\int_0^L \bar{\rho}(x) A(x-y)\, dx - \frac{\sigma^2}{\bar{\rho}(y)^2} R'\Big(\frac{\sigma}{\bar{\rho}(y)}\Big) = \Lambda(y), \tag{3.11}$$

where $\Lambda(y)$ is a constant function of y. The repulsive term in Equation 3.10 is contant in y because $\bar{\rho}(y)$ is constant. The integral of attraction can be shown also to be constant in y. Consider a substitution such that $x - y = z$ and $dx = dz$. Then the integral becomes,

$$\int_0^L \bar{\rho}(y+z) A(z)\, dz, \tag{3.12}$$

where $\bar{\rho}(y+z)$ is still a constant and $A(z)$ is a periodic function for $0 < z < L$ so that the integral results in a constant in y. Thus, we have shown that if $\bar{\rho}(x)$ is a constant function, then it is an equilibrium of the energy functional defined in Equation 3.7.

For the constant density equilibrium to be stable, W_2 must be greater than zero. The second variation is given by,

$$\begin{aligned} W_2[\bar{\rho},\tilde{\rho}] &= \int_0^L \tilde{\rho}(x)^2\left[\frac{\sigma^2}{\bar{\rho}^3}R'\Big(\frac{\sigma}{\bar{\rho}}\Big)+\frac{\sigma^3}{2\bar{\rho}^4}R''\Big(\frac{\sigma}{\bar{\rho}}\Big)\right]dx+\frac{1}{2}\int_0^L\int_0^L \tilde{\rho}(x)\tilde{\rho}(y)A(x-y)\,dxdy \\ &= \int_0^L \tilde{\rho}(x)^2\big[B\big]\,dx+\frac{1}{2}\int_0^L\int_0^L \tilde{\rho}(x)\tilde{\rho}(y)A(x-y)\,dxdy, \end{aligned} \tag{3.13}$$

where B is a constant. To arrive at stability conditions, we must use a Fourier series approximation of the perturbation $\tilde{\rho}(x)$. Suppose,

$$\tilde{\rho}(x) = \sum_{n=1}^{\infty} a_n \cos\Big(\frac{2n\pi}{L}x\Big)+b_n\sin\Big(\frac{2n\pi}{L}x\Big). \tag{3.14}$$

The first term of Equation 3.13 can be expressed in terms of an L^2-inner product such that,

$$\begin{aligned} W_2^R[\bar{\rho},\tilde{\rho}] &= B\int_0^L \tilde{\rho}(x)^2\,dx = B\big\langle\tilde{\rho}(x),\tilde{\rho}(x)\big\rangle \\ &= B\sum_{n=1}^{\infty}\sum_{m=1}^{\infty}\left[a_na_m\Big\langle\cos\Big(\frac{2n\pi}{L}x\Big),\cos\Big(\frac{2m\pi}{L}x\Big)\Big\rangle+b_nb_m\Big\langle\sin\Big(\frac{2n\pi}{L}x\Big),\sin\Big(\frac{2m\pi}{L}x\Big)\Big\rangle\right] \\ &= B\sum_{n=1}^{\infty}\sum_{m=1}^{\infty}\frac{L}{2}\Big[a_na_m\delta_{nm}+b_nb_m\delta_{nm}\Big] \\ &= B\sum_{n=1}^{\infty}\frac{L}{2}\Big(a_n^2+b_n^2\Big) \end{aligned}$$

Now consider the second term of Equation 3.13 where $A(r)$ can also be re-expressed as a Fourier series. Because the attractive potential is an even periodic function, it has a cosine series approximation, such that

$$A(x-y) = \frac{c_0}{2}+\sum_{j=1}^{\infty} c_j\cos\Big(\frac{2j\pi}{L}(x-y)\Big). \tag{3.15}$$

Using an angle-sum trigonometric identity, the series can be written as,

$$A(x-y) = \frac{c_0}{2} + \sum_{n=1}^{\infty} c_j \Big[\cos\Big(\frac{2j\pi}{L}x\Big)\cos\Big(\frac{2j\pi}{L}y\Big) + \sin\Big(\frac{2j\pi}{L}x\Big)\sin\Big(\frac{2j\pi}{L}y\Big)\Big].$$

The attractive term of $W_2[\bar{\rho}, \tilde{\rho}]$ becomes a large expression,

$$\begin{aligned} W_2^A[\bar{\rho}, \tilde{\rho}] = \frac{1}{2}\sum_{n=1}^{\infty}\sum_{m=1}^{\infty}\sum_{j=1}^{\infty}\Bigg[&\int_0^L\int_0^L \frac{c_0}{2}\Big(a_n\cos\Big(\frac{2n\pi}{L}x\Big) + b_n\sin\Big(\frac{2n\pi}{L}x\Big)\Big)\,dxdy \\ &+ \int_0^L\int_0^L c_j\Big(a_n\cos\Big(\frac{2n\pi}{L}x\Big) + b_n\sin\Big(\frac{2n\pi}{L}x\Big)\Big)\cos\Big(\frac{2j\pi}{L}x\Big)\cos\Big(\frac{2j\pi}{L}y\Big)\,dxdy \\ &+ \int_0^L\int_0^L c_j\Big(a_n\cos\Big(\frac{2n\pi}{L}x\Big) + b_n\sin\Big(\frac{2n\pi}{L}x\Big)\Big)\sin\Big(\frac{2j\pi}{L}x\Big)\sin\Big(\frac{2j\pi}{L}y\Big)\,dxdy\Bigg], \end{aligned}$$

that can be simplified massively by evaluating the terms as inner products. The first double integral vanishes because each trigonometric function is integrated independently over a full period. So, the attractive term of second variation is,

$$\begin{aligned} W_2^A[\bar{\rho}, \tilde{\rho}] &= \frac{L^2}{8}\sum_{n=1}^{\infty}\sum_{m=1}^{\infty}\sum_{j=1}^{\infty} c_j\Big(a_n a_m \delta_{jn}\delta_{jm} + b_n b_m \delta_{jn}\delta_{jm}\Big) \\ &= \sum_{n=1}^{\infty}\frac{c_n L^2}{8}\Big(a_n^2 + b_n^2\Big). \end{aligned}$$

Finally, the complete second variation is,

$$W_2[\bar{\rho}, \tilde{\rho}] = \frac{L}{2}\sum_{n=1}^{\infty}\Big(B + \frac{c_n L}{4}\Big)\Big(a_n^2 + b_n^2\Big). \tag{3.16}$$

With this equation, we can evaluate the stability of the constant density equilibrium solution, $\bar{\rho}$. The stability of constant density to the k^{th} Fourier mode of the perturbation is given by the sign of,

$$\Big(B + \frac{c_k L}{4}\Big).$$

When the expression is positive, it is a stable mode and, when negative, an unstable mode.

Chapter 4

Numerical Results

4.1 Potential energy functions

First, we consider a class of potential energy function called the Morse potential which is characterized by short ranged repulsion and long ranged attraction while being asymptotic to zero. These properties make it such that two particles interacting flow to the minimum of the potential at intermediate values of r. One such function is

$$Q(r_{ij}) = e^{-|r_{ij}|} - FDe^{-|r_{ij}|/D}, \tag{4.1}$$

where $r_{ij} = x_i - x_j$, F is a parameter of attraction strength, and D is a parameter for the length scale of attraction. The function has two terms: the first is the repulsive contribution, $R(r_{ij}) = e^{-|r_{ij}|}$ and the second is the attractive contribution, $A(r_{ij}) = -FDe^{-|r_{ij}|/D}$. Notice that repulsion is nonzero over the entire interval which is why we consider this to be a "global" repulsion function but we refer to it as Morse repulsion.

In a previous thesis by Quentin Barth (2019), this interaction potential was periodicitized to the interval between $[0, L]$. His result is that the potential between any two individuals i and j is

$$\begin{aligned}\tilde{Q}(r_{ij}) &= \sum_{n=-\infty}^{\infty} Q(x_i - (x_j + nL)) \\ &= \frac{\cosh\left(L/2 - \mid r_{ij} \mid\right)}{\sinh(L/2)} - FD\frac{\cosh\left(\frac{L/2-|r_{ij}|}{D}\right)}{\sinh\left(\frac{L}{2D}\right)} \qquad r_{ij} \in [0, L],\end{aligned} \tag{4.2}$$

such that i is effected by an infinite amount of mirrors of particle j outside the boundary. This allows us to simulate large swarms while ignoring edge effects. With a substitution of $r^* = r - L\lfloor r/L \rfloor$, the function $\tilde{Q}(r^*)$ is fully periodic for use in numerical simulation. Note that $\tilde{Q}(r^*)$ is even such that $\tilde{Q}(r^*) = \tilde{Q}(-r^*)$ and periodic such that $\tilde{Q}(r^* + L) = \tilde{Q}(r^*)$.

Secondly, we use the same Morse attraction function, $A(r)$, as above but construct a repulsion function $R(r)$ that is singular at the origin and has a parameter that varies the length over which repulsion is nonzero. This singular repulsive potential must have a continuous first derivative with compact support such that the repulsive "force" reaches and remains at zero at some point $x = L_r < L$. One such function we created is

$$R'(r) = -p\Big(\frac{1}{L_r}\Big)^{1+p}\Big(\frac{L_r}{r}\Big)^{1+p}\Big(1 - \frac{r}{L_r}\Big)H\big(L_r - r\big),$$

where p is the exponent of $\frac{1}{r}$ and $H\big(L_r - r\big)$ is the Heaviside function that becomes zero for $r > L_r$. Now we can integrate this function to find our repulsive energy

$$\begin{aligned} R(r) &= -p\Big(\frac{1}{L_r}\Big)^{1+p}\int_{\infty}^{r}\Big(\frac{L_r}{z}\Big)^{1+p}\Big(1 - \frac{z}{L_r}\Big)H\big(L_r - z\big)dz \\ &= L_r^{-p}\left[\Big(\frac{L_r}{r}\Big)^{p} + \frac{p}{1-p}\Big(\frac{L_r}{r}\Big)^{p-1} - \frac{1}{1-p}\right]H\big(L_r - r\big). \end{aligned} \tag{4.3}$$

We consider this kind of repulsive potential to be "local" even though the function is well defined globally because L_r determines some radius within which particles repel each other. We call this the singular repulsion function. In all of our analyses using singular repulsion, we set $p = 2$.

4.2 Stability in discrete model

4.2.1 Global repulsion

In Chapter 2 we derived Equation 2.16, an analytical expression for the eigenvalues of the Hessian of our system at an even spacing equilibrium. Using our Morse potential, the eigenvalue equation becomes

$$\lambda^{(k)} = 2\sum_{\ell=1}^{M}\left[\frac{\cosh\left(L/2 - \ell\Delta\right)}{\sinh(L/2)} - \frac{F}{A}\frac{\cosh\left(\frac{L/2-\ell\Delta}{A}\right)}{\sinh\left(\frac{L}{2A}\right)}\right]\Big(1 - \cos\Big(\frac{2\pi}{N}\ell k\Big)\Big).$$

In this case, attractive and repulsive potential functions are effective globally. We numerically evaluate this result in MATLAB in two ways. Firstly, we build our Hessian and call an built-in function for the eigenvalues of a matrix. Then, we apply the Fast Fourier Transform (FFT) to the first row vector of the Hessian. We compare these two sets of eigenvalues against the results of our analytic expression to find that they agree for various numbers of individuals as long as N is an odd integer. As a measure of verification of the analytical eigenvalues, we sort the vectors and return the maximum absolute value of the difference between the vectors. The analytical equation has a maximum difference with the numerical eigenvalues on the order of 10^{-15} using both the FFT and eig() functions for $N = 51$.

We also find the transition to instability of constant density predicted by our eigenvalue equation as the strength of attraction increases. In Figure 4.1, we see that the set of eigenvalues is positive definite for $F < 0.4483$ and contains at least one negative eigenvalue for greater values of F.

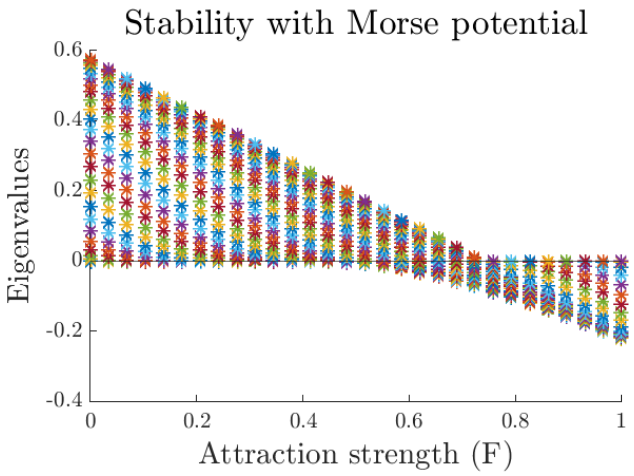

Figure 4.1 The strength of attraction, F, is on the x-axis in discrete steps and the resulting eigenvalues from Equation 2.16 with Morse potential are on the y-axis. The set of parameters used is $N = 51$, $L = 100$, and $D = 1.5$. The values of F we use are 30 evenly spaced points between 0 and 1.

Furthermore, we use an optimization routine in MATLAB to compare the bifurcation point to instability of even spacing as F increases with that predicted by our analytical equation. We use the fmincon() function to find the vector of positions that minimizes the energy at the given parameter values. In this case we use parameters, $N = 15$, $L = 20$, and $D = 10$. We

find that the optimization routine predicts a transition from even spacing to a clumped state at $F = 0.0963$ while our analytical equation predicts the instability to lie at $F = 0.0955$ for the same parameters.

4.2.2 Local repulsion

Now we use Morse attraction and the repulsion function defined by Equation 4.3 as the terms of our pairwise potential energy. Repeating the analysis of the previous section, we verify the analytical equation with singular repulsion against the FFT and eig() functions. We find that the maximum of the difference between vectors is on the order of 10^{-13}, which means that our analytical eigenvalues agree very well with numerical counterparts. We can also see by comparing Figure 4.1 and Figure 4.2 that even spacing becomes unstable more quickly with singular repulsion at $F = 0.2069$.

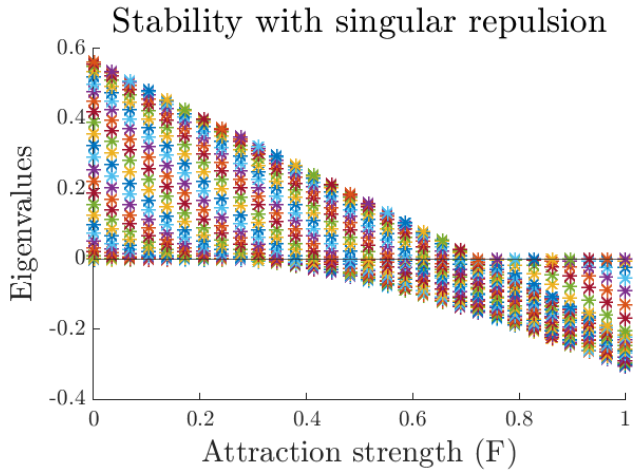

Figure 4.2 The strength of attraction, F, is on the x-axis in discrete steps and the resulting eigenvalues from Equation 2.16 with Morse attraction and singular repulsion are on the y-axis. The set of parameters used is $N = 51$, $L = 100$, $D = 1.5$, and $L_r = 2$. The values of F we use are 30 evenly spaced points between 0 and 1.

Next, we compare bifurcation points between the analytical equation and our optimization routine with singular repulsion. We use parameters, $N = 15$, $L = 20$, $D = 10$, and $L_r = 6$. We find that the optimization routine predicts a transition from even spacing to a clumped state at $F = 0.2601$ while our analytical equation predicts the instability to lie at $F = 0.2613$ for

the same parameters. As an example, Figure 4.3 shows the optimal particle configurations for each value of F.

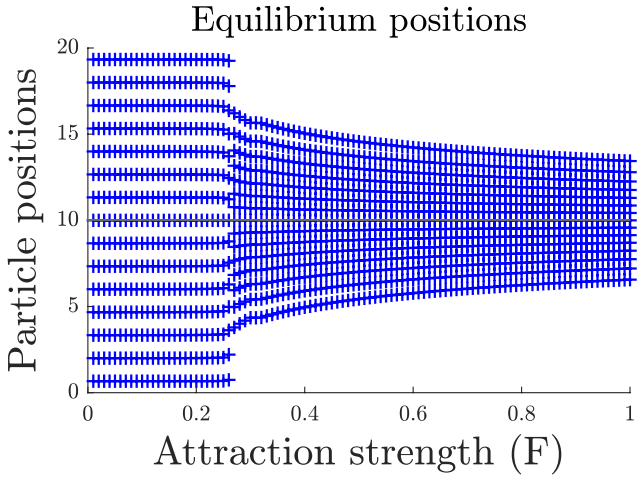

Figure 4.3 The strength of attraction, F, is on the x-axis in discrete steps and the optimal particle positions with Morse attraction and singular repulsion are on the y-axis. The set of parameters used is $N = 15$, $L = 20$, $D = 10$, and $L_r = 6$. The values of F we use are 30 evenly spaced points between 0 and 1. Notice how the particles transition from even spacing to clumped in our optimization routine.

4.2.3 Hysteresis

We use our optimization routine with Morse and singular repulsion to investigate whether there is evidence of hysteresis in the system with respect to attraction strength. Hysteresis is when the state of a system depends on the history or trajectory of its parameters as they change. In our case, we vary the attraction strength in ascending and descending order to see whether the transition between clumped and constant density states are at different values of F. To ensure that the direction of F is taken into account, we use the method of continuation wherein the initial condition of the optimization routine is redefined to be near the optimal solution for the previous value of F. If $\vec{x}_{current}$ is the equilibrium at the current value of F and $\vec{x}_{previous}$ is the equilibrium for the previous value, then the initial condition for the next value of F will be the tangent line approximation, $x_0 = 2\vec{x}_{current} - \vec{x}_{previous}$. Because our state space is large with N particles, we demonstrate hysteresis by measuring the size of the swarm.

We find hysteresis with both Morse and singular repulsion. Under Morse repulsion, even spacing is stable for $F < 0.0964$ when ascending and stable for $F < 0.089$ when descending. The difference between bifurcation points is less than 0.01. By contrast, under singular repulsion, even spacing is stable for $F < 0.2602$ when ascending and stable for $F < 0.22$ when descending. In this case the difference between bifurcation points is about 0.04. In Figure 4.4, we see the differences between ascending and descending F on the size of the swarm with Morse repulsion. We use a higher density of points near the transition to resolve clearly where the bifurcation occurs in each case. In Figure 4.5, we see the same hysteresis analysis for singular repulsion. Notice that the x-axis on Figure 4.4 ranges between $F = 0$ and $F = 0.5$. When $F = 1$ and $D = 10$, Morse attraction is sufficiently strong to collapse the swarm to a single point where the size of the swarm is on the order of 10^{-11}. Using singular repulsion however, the potential function diverges to infinity at the origin such that the particles within repulsion range of each other are repelled much stronger. The size of the swarm doesn't reach 1 until $F = 200$.

4.3 Stability in continuum model

The most significant result that can be demonstrated numerically with our continuum model is that the constant density minimizer of our energy functional, $W[\bar{\rho}]$, becomes unstable when the total mass of the swarm crosses some threshold. This is an important feature of our model because locusts are observed to transition from homogeneous to clumped states of organization when they increase passed a threshold of average density. Remember that we derived our continuum model such that any repulsive potential energy used is only applied to an agent's two nearest neighbors so we can test both the Morse and singular repulsion functions operating locally. First, with singular repulsion, we get the expected result. When the total mass is low, there are no unstable Fourier modes of an arbitrary perturbation. In Figure 4.6, the smallest wavenumber is the first to become unstable and the bifurcation occurs at an average density of 0.29 at the given parameters. However, if we use Morse repulsion, the stability boundary is very different. Instead, small wavenumbers are all unstable and, at some high density, all wavenumbers are stable.

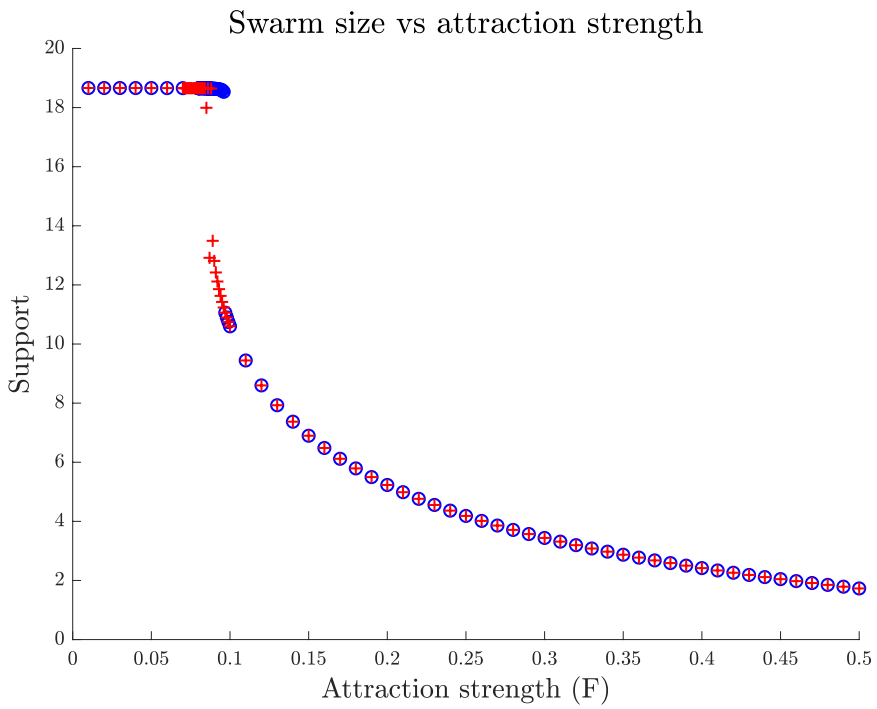

Figure 4.4 Potential energy is Morse attraction and Morse repulsion. Blue circles correspond to the equilibrium swarm size as F is iterated in ascending order, while red crosses correspond to swarm sizes as F is iterated in reverse. The set of parameters used is $N = 15, L = 20$, and $D = 10$. We can see that the bifurcation to instability of even spacing occurs at a slightly higher value when F is ascending rather than descending.

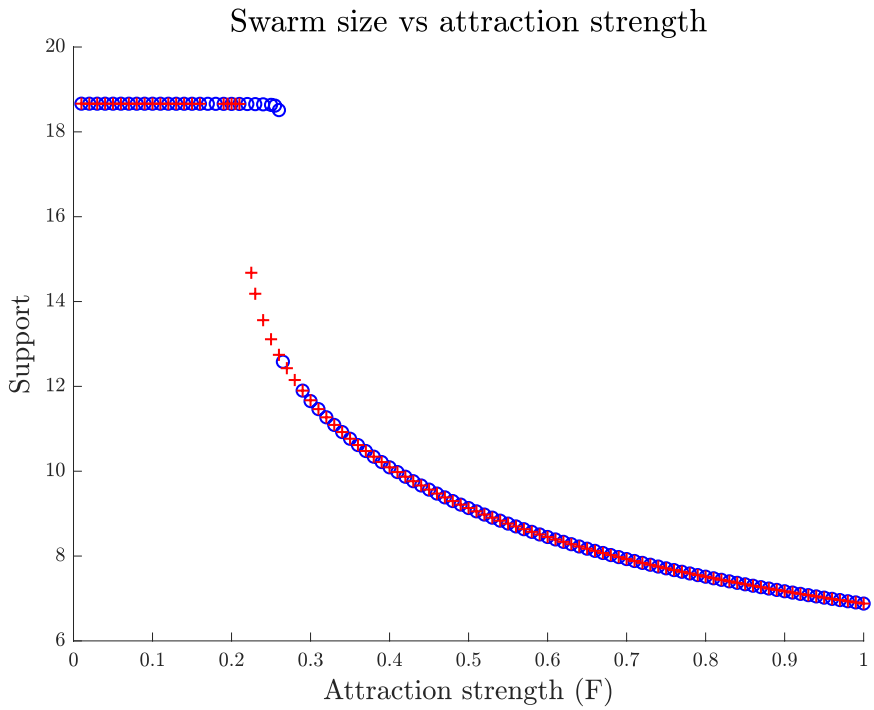

Figure 4.5 Potential energy is Morse attraction and singular repulsion. Blue circles correspond to the equilibrium swarm size as F is iterated in ascending order, while red crosses correspond to swarm sizes as F is iterated in reverse. The set of parameters used is $N = 15$, $L = 20$, $D = 10$, and $L_r = 6$. We can see that the bifurcation to instability of even spacing occurs at a slightly higher value when F is ascending rather than descending.

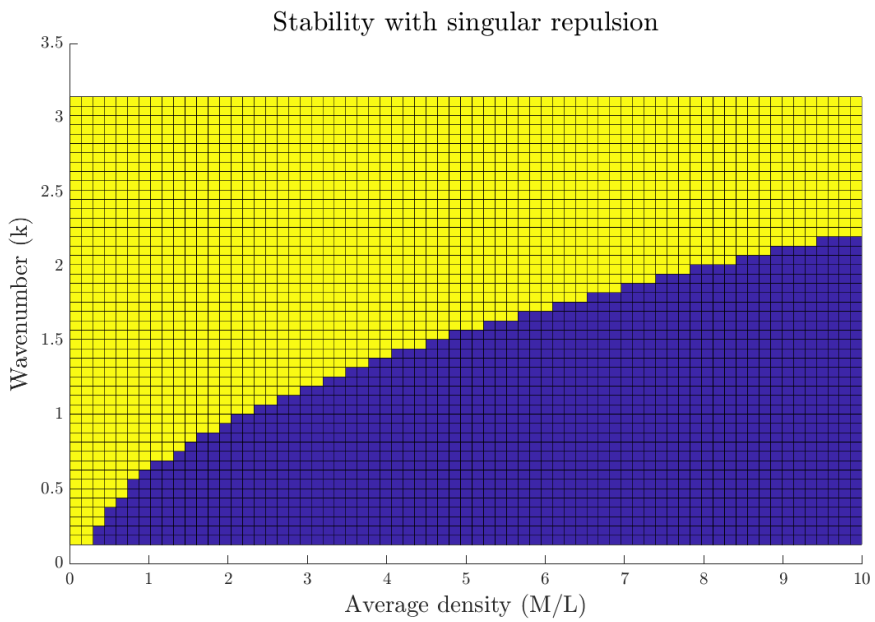

Figure 4.6 Stability of constant density as a function of wavenumber and average density. A yellow square indicates a stable mode at that average density and wavenumber, while purple indicates instability. In this figure we use singular repulsion and Morse attraction with parameters $L = 100$, $D = 3$, $F = 0.25$, $L_r = 20$, and $\bar{\rho} = 10$.

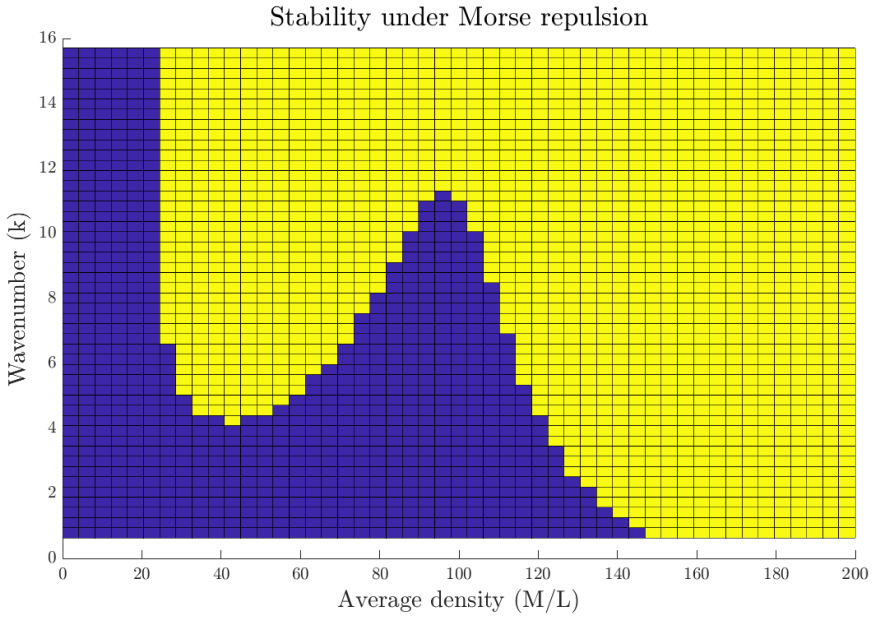

Figure 4.7 Stability of constant density as a function of wavenumber and average density. The yellow region indicates stable modes of average density and wavenumber, while purple region indicates instability. In this figure we use Morse repulsion and Morse attraction with parameters $L = 20$, $D = 1.5$, $F = 0.25$, and $\bar{\rho} = 10$.

Chapter 5

Conclusion

In this thesis, we investigate a first order model of particle interactions under a general pairwise potential energy, $Q(r)$, in a one dimensional periodic domain. Formulating the problem as energy minimization, we are able to find and analyze the stability of the constant density or evenly spaced equilibrium of the swarm. We derive an analytical expression for the eigenvalues of this system that determine the stability of even spacing under various parameter conditions.

We test our results with two interaction potentials. First, a Morse potential given by Equation 4.2. Secondly, a potential in which the repulsive term in Equation 4.2 is exchanged for $R(r)$ defined by Equation 4.3. This function $R(r)$ is constructed to have a variable, L_r, determining the range over which the repulsive force is nonzero. We are interested in this kind of repulsion because, with a Morse potential, repulsion is effective between all agents and this is nonbiological. Our new repulsive term is singular at the origin and can be made to operate locally.

We find that there are two equilibria for our system, even spacing and clumped configurations. Our eigenvalue expression predicts that the even spacing configuration has a bifurcation to instability as attraction strength increases. We verify this bifurcation result with an optimization routine to find the energy minimizing configurations of the swarm at various values of F. Using this optimization routine, we demonstrate a weak hysteretic effect on the equilibrium configuration of the swarm with respect to attraction strength F.

From this discrete model of particles swarming in one dimension, we derive its continuum analogue as an energy functional with energy minimizing density distributions. In this case, we use calculus of variations

to determine the stability of a constant density solution. Using singular repulsion, we find that all possible wavenumbers of an arbitrary perturbation to equilibrium are stable and, as total mass increases, there is a bifurcation to instability. If you would like more information on our numerical results and simulations, please visit my GitHub repository contain all files used: https://github.com/miguelvelezz/thesis.

In the future, I plan to work on verifying my results against the work of other researchers attempting to create swarming models with local repulsion. Principally, Burger et al. (2014) construct a continuum swarming model with nonlinear local repulsion.

Bibliography

Barth, Quentin. 2019. Swarm stability: Distinguishing between clumps and lattices. *HMC Senior Theses* (227).

Bernoff, Andrew J, and Chad M Topaz. 2011. A primer of swarm equilibria. *SIAM Journal on Applied Dynamical Systems* 10(1):212–250.

Burger, Martin, Razvan Fetecau, and Yanghong Huang. 2014. Stationary states and asymptotic behavior of aggregation models with nonlinear local repulsion. *SIAM Journal on Applied Dynamical Systems* 13(1):397–424.

Karner, Herbert, Josef Schneid, and Christoph W Ueberhuber. 2003. Spectral decomposition of real circulant matrices. *Linear Algebra and Its Applications* 367:301–311.